Acta Cryst. (1983). B**39**, 227–235

Protonic Solid Electrolytes: A Single-Crystal Neutron Diffraction Study of Ammonium–Hydronium β''-Alumina

By John O. Thomas

Institute of Chemistry, University of Uppsala, Box 531, *S*-751 21 *Uppsala, Sweden*

and Gregory C. Farrington

Department of Materials Science and Engineering, University of Pennsylvania, Philadelphia, PA 19104, *USA*

(*Received* 2 *November* 1981; *accepted* 10 *November* 1982)

Abstract

The structure and ionic distribution in the conducting plane of ammonium–hydronium β''-alumina, a solid electrolyte with high protonic conductivity, have been determined by single-crystal neutron diffraction. The composition, constrained in the refinement to neutrality, is: $(NH_4^+)_{1\cdot56}(H_3O^+)_{0\cdot19}Mg_{0\cdot75}Al_{10\cdot25}O_{17}.(H_2O)_{0\cdot25}$, with three such units per unit cell. The hexagonal cell dimensions are: $a = 5\cdot6310\,(4)$, $c = 34\cdot378\,(6)$ Å, $V = 944\cdot0$ Å^3, for the rhombohedral space group $R\bar{3}m$. $R(F^2) = 0\cdot035$, $R_w(F^2) = 0\cdot049$ for 1505 reflections. The structure comprises spinel blocks of Al atoms, tetrahedrally or octahedrally coordinated to O atoms. One of the two tetrahedrally coordinated Al^{3+} sites is occupied to 37% by Mg^{2+} to provide charge compensation in the structure. The site Al(2) is near the centre of the spinel block ($z \sim 0$). The NH_4^+ ions occupy 6(c) sites in the conducting planes which interleave the spinel blocks at $z = \pm\frac{1}{6}$ and $\frac{1}{2}$, with a partial site occupation of 78%. When such sites are not occupied by NH_4^+ ions, they are occupied by either an H_2O molecule or an H_3O^+ ion, with a statistical ratio between the two of 4:3. The distance from the O atom of the H_2O molecule or H_3O^+ ion to the $\bar{3}$ axis is 0·84 (1) Å. Site-occupation considerations suggest a Grotthus-type mechanism for proton transfer involving three components: rotational translation of H_3O^+ and H_2O, and proton transfer from H_3O^+ to H_2O.

Introduction

Solid electrolytes with high conductivities for protons are rare. Protons are such strong electrophiles that they are trapped in crystalline solids by nucleophilic groups High proton conductivity in the solid state requires a Grotthus-like network of donor/acceptor groups (Shilton & Howe, 1979). Well known solid electrolytes with high proton conductivities include H_3OClO_4 (Potier & Rousselet, 1973) and $HUO_2PO_4.4H_2O$ (Shilton & Howe, 1977), which have conductivities of about 10^{-4} Ω^{-1} cm^{-1} at 298 K. In both, protons diffuse through $H^+(H_2O)_x$ networks, and a high water content is essential for rapid proton transport. Consequently, dehydration dramatically decreases the conductivity of each.

The few good proton conductors that are known, such as $HUO_2PO_4.4H_2O$, typically dehydrate at 373 K or lower, considerably below the 473–673 K temperature range in which they might be used as electrolytes in novel fuel cells. The challenge in finding a technologically useful solid electrolyte for protons therefore involves not only identifying a material with an intrinsically high proton conductivity, but one which maintains its composition and conductivity to relatively high temperatures.

One class of solid proton conductors which do retain their compositions to at least 473–498 K is that of the protonic β- and β''-aluminas. Several of these compounds have unusually high protonic conductivities. This paper presents the first detailed investigation of the structure of one of the most conductive protonic β''-aluminas, ammonium–hydronium β''-alumina $(NH_4)_{1\cdot67-y}(H_3O)_yMg_{0\cdot67}Al_{10\cdot33}O_{17}.(H_2O)_x$. Its ionic conductivity is about 10^{-3} Ω^{-1} cm^{-1} at 298 K.

Protonic β- and β''-aluminas are prepared by the ion exchange of sodium β-alumina ($Na_{1\cdot15}Al_{11}O_{17\cdot07}$) and sodium β''-alumina ($Na_{1\cdot67}Mg_{0\cdot67}Al_{10\cdot33}O_{17}$). Exchange in concentrated sulphuric acid produces hydronium compositions in which each Na^+ ion has been replaced by a proton and associated water of hydration. The preparation (Breiter, Farrington, Roth & Duffy, 1977), stability (Roth, Breiter & Farrington, 1978) and conductivity (Farrington, Briant, Breiter & Roth, 1978) of hydronium β-alumina $[(H_3O)_{1\cdot24}Al_{11}O_{17\cdot12}]$ have been previously discussed. Results of a similar investigation of hydronium β''-alumina have also been presented (Farrington & Briant, 1978). Both compounds retain their water of hydration to at least 473 K, at which temperature they undergo reversible partial dehydrations. Upon further heating, the basic

0567-7408/83/020227-09$01.50

structure of β-alumina is retained to about 873–973 K and that of β''-alumina to about 673 K. Both compounds are unusually stable protonic solid electrolytes. However, their conductivities differ greatly. The conductivity of hydronium β-alumina is about 10^{-11} Ω^{-1} cm^{-1} at 298 K and 10^{-7} Ω^{-1} cm^{-1} at 473 K; that of hydronium β''-alumina is 10^{-3} to 10^{-6} Ω^{-1} cm^{-1} at 298 K.

Ammonium derivatives of both β- and β''-alumina can be prepared by ion exchange in molten NH_4NO_3. Single crystals of sodium β-alumina immersed in molten NH_4NO_3 at 473 K undergo rapid ion exchange in which each sodium ion is replaced by an ammonium ion. Ammonium β-alumina has a conductivity of 10^{-6} Ω^{-1} cm^{-1} at 298 K. It increases with an activation energy of 0·5 eV (1 eV $\equiv 1{\cdot}60 \times 10^{-19}$ J) until about 623 K, at which temperature NH_4^+ ions dissociate into H^+ and NH_3, and NH_3 is lost from the crystals (Hooper, Tofield & Sampson, 1979).

Similar immersion of sodium β''-alumina crystals in molten ammonium nitrate yields a different and unexpected composition in which a mixture of NH_4^+, H_3O^+ ions and H_2O molecules replace sodium in the structure. These compounds have the general formula $(NH_4)_{1\cdot67-y}(H_3O)_yMg_{0\cdot67}Al_{10\cdot33}O_{17}.(H_2O)_x$, and have been referred to as ammonium–hydronium (NH_4^+–H_3O^+) β''-alumina. The exact composition resulting from a particular exchange appears to depend upon the size of the crystals which are being exchanged and the temperature and extent of hydration of the ammonium nitrate. In one set of experiments, sodium β''-alumina crystals measuring about 1 × 2 × 0·2 mm were immersed in molten ammonium nitrate at 473 K for 8–15 days. The average composition of the products of these exchanges was $(NH_4)_{1\cdot0}(H_3O)_{0\cdot67}Mg_{0\cdot67}Al_{10\cdot33}O_{17}$.

Upon heating, ammonium–hydronium β''-alumina undergoes a series of reversible and irreversible composition changes which are summarized below.

$$\begin{gathered}
(NH_4)_{1\cdot67-y}(H_3O)_yMg_{0\cdot67}Al_{10\cdot33}O_{17}.(H_2O)_x \\
\uparrow\downarrow \ \text{503–603 K} \\
H_{1\cdot67}Mg_{0\cdot67}Al_{10\cdot33}O_{17} + (x+y)H_2O + (1{\cdot}67-y)NH_3 \\
\downarrow \ \text{653–773 K} \qquad\qquad (1) \\
H_{0\cdot33}Mg_{0\cdot67}Al_{10\cdot33}O_{16\cdot33} + 0{\cdot}67H_2O \\
\downarrow \ \text{873–1173 K} \\
Mg_{0\cdot67}Al_{10\cdot33}O_{16\cdot17} + 0{\cdot}16H_2O
\end{gathered}$$

The conductivity of ammonium–hydronium β''-alumina is unusually high, perhaps the highest of the protonic β/β''-aluminas. No systematic study of its conductivity as a function of composition has been reported. However, crystals with the composition $(NH_4)_{1\cdot0}(H_3O)_{0\cdot67}Mg_{0\cdot67}Al_{10\cdot33}O_{17}$ have conductivities of about 10^{-3} Ω^{-1} cm^{-1} at 298 K and nearly 10^{-2} Ω^{-1} cm^{-1} at 473 K (Farrington & Briant, 1979). The conductivity decreases dramatically upon dehydration and deammoniation.

The existence of ammonium–hydronium β''-alumina poses several interesting questions:

(*a*) Why does a mixed NH_4^+–H_3O^+ composition form at all during ion exchange in molten NH_4NO_3? Some hydronium-ion activity must exist in the molten salt as a result of its water of hydration and the protons formed by slow decomposition. However, the activity of H_3O^+ is surely much less than that of NH_4^+.

(*b*) What is the mechanism of conductivity in NH_4^+–H_3O^+ β''-alumina; specifically, the relative contributions of discrete NH_4^+ and H_3O^+ diffusion compared to Grotthus-like H^+ hopping?

(*c*) Why do sodium β- and sodium β''-alumina exchange in NH_4NO_3 to form compounds with such different compositions and conductivities?

To begin to answer these questions, we have investigated the structure and the distribution of the mobile ions in NH_4^+–H_3O^+ β''-alumina by single-crystal neutron diffraction. Before discussing the details of this study, however, we briefly review the structures of sodium β- and sodium β''-aluminas.

Sodium β- and β''-aluminas are non-stoichiometric sodium aluminates whose compositions are variations of the ideal formula $NaAl_{11}O_{17}$. Each compound contains more sodium than this formula indicates. The two compounds differ partly in the mechanism by which the charge of this excess sodium is compensated. In β-alumina, additional oxygen ions compensate the excess sodium content. In β''-alumina, compensation is achieved by substituting divalent (*e.g.* Mg^{2+}, Ni^{2+}) or monovalent (*e.g.* Li^+) ions for trivalent Al^{3+} species in the structure. The general formula for sodium β-alumina is $Na_{1+x}Al_{11}O_{17+x/2}$, where x is typically 0·1 to 0·3. In the Mg-compensated form used in this study, β''-alumina has the general formula $Na_{1+x}Mg_xAl_{11-x}O_{17}$. The range of x appears to be quite small. Most Mg-stabilized β''-alumina compositions reported are essentially the same as that used in this study, $Na_{1\cdot67}Mg_{0\cdot67}Al_{10\cdot33}O_{17}$.

Compositions of β- and β''-aluminas containing mobile ions other than sodium are nearly always prepared by ion exchange. The protonic forms are prepared by ion exchange in aqueous acids, in molten ammonium nitrate, or by the reduction of silver β-alumina with hydrogen. The time required for complete ion exchange is influenced by the rate of migration of the replacing ion. For example, lithium β-alumina can be prepared from 2 × 1 × 0·5 mm single crystals of sodium β-alumina within 30–60 min at 923 K in LiCl (Briant & Farrington, 1981). In contrast, the preparation of comparably sized hydronium (H_3O^+) β-alumina crystals from sodium β-alumina requires immersion in concentrated sulphuric acid for 2–3 weeks at 573 K (Breiter, Farrington, Roth & Duffy, 1977).

The β- and β''-aluminas crystallize in layered structures. The layers comprise spinel-type blocks of Al and O atoms which are linked together by Al—O—Al bridging bonds to define relatively open conducting regions in which the mobile ions are found. Ionic conductivity occurs in two dimensions within the conducting regions. More complete discussions of the β and β'' structures appear elsewhere (Bettman & Peters, 1969; Peters, Bettman, Moore & Glick, 1971; Roth, 1972; Roth, Reidinger & La Placa, 1976).

Experimental

A single crystal suitably large for neutron diffraction was obtained by the ion exchange of an Na^+ β''-alumina crystal for 45 days in molten NH_4NO_3 (see *Introduction*).* The volume of the crystal used was 29 mm^3.

Prior to the neutron data collection, a small flake of the crystal was removed (the crystals are very micaceous), mounted on a CAD-4 automatic X-ray diffractometer, and the θ values of 25 reflections determined. The hexagonal cell parameters quoted in the *Abstract* were refined by a least-squares procedure.

The neutron crystal was washed in alcohol and vacuum dried [at ~0·5 mm Hg (~$0{\cdot}7 \times 10^2$ Pa)] at ambient temperature prior to mounting on an aluminium pin with a minimal quantity of Araldite epoxy resin. The crystal was quickly encapsulated in a thin-walled quartz-glass tube to protect it from further water uptake. Data were collected at 295 K with an automatic Hilger & Watts four-circle diffractometer at the *R*2 reactor at Studsvik, Sweden. The neutron flux at the crystal was $1{\cdot}26 \times 10^6$ n cm^{-2} s^{-1} at a wavelength of 1·21 Å.

Working initially with a hexagonal cell, a preliminary set of reflections was collected for $+h$, $+k$, $+l$ out to $\theta = 20°$, with an $\omega/2\theta$ step scan. The intensities of reflections expected to be absent on the basis of the assumed space group $R\bar{3}m$ (*i.e.* $-h + k + l \neq 3n$ reflections in the hexagonal cell) were included in the measurement. None was found to have an intensity significantly above the background, and all could thus be safely eliminated from the data collection. The full data collection could then proceed in the rhombohedral cell for reflections $+h$, $+k$, $\pm l$ out to $\sin\theta/\lambda = 0{\cdot}693$ Å^{-1}. The intensities of three test reflections chosen to monitor the data collection were found to display no more than statistically insignificant random variations throughout the data collection.

In anticipation of the presence of anisotropic secondary extinction effects in the data (ubiquitous in single-crystal neutron data), no symmetry averaging was performed on the measured intensities. Despite this, a total of 36 strong, severely extinction affected reflections were subsequently removed from the data set (see *Refinement*). The observed intensities were corrected for background (Lehmann & Larsen, 1974), Lorentz and absorption effects. The linear absorption coefficient used in the latter was measured experimentally to 130 m^{-1}, corresponding to 56·8 b (1 b $\equiv$ 100 fm^2) for the incoherent scattering cross-section of H. The calculated transmission values fall in the range 0·61–0·89.

The resulting set of F_o^2 values were assigned standard deviations $\sigma_c(F_o^2)$ calculated from $\sigma_c(I_o)$ on the basis of assumed Poisson counting statistics.

The refinements

All refinements were made in the full-matrix least-squares program *UPALS* (Lundgren, 1979) by minimizing the function $\sum w(|F_o|^2 - |F_c|^2)$, where $w = 1/\sigma^2(F_o^2)$ and $\sigma^2(F_o^2) = \sigma_c^2(F_o^2) + (kF_o^2)^2$. The value of k used was 0·01, and was that found empirically to result in the most even distribution of $w(F_o^2 - F_c^2)^2$ values across incremental ranges of $|F_o^2|$ and $\sin\theta/\lambda$ values. All reflections with $F_o^2 < 2\sigma(F_o^2)$ were removed from the refinements. A total of 1505 reflections were used in the final refinements. The coherent scattering amplitudes used throughout were those taken from *International Tables for X-ray Crystallography* (1974). The sequence of refinements and subsequent Fourier calculations require a detailed description.

Phase 1

The refinements were begun using the atom positions for the spinel-block structure [including column oxygen O(5)] found for Na^+ β''-alumina by Bettman & Peters (1969). It was found necessary to refine anisotropic temperature factors and an isotropic extinction parameter to achieve convergence. Subsequent refinement of the occupancy of the Al sites indicated unequivocally that *only the* Al(2) *site* was occupied (to 37%: see Table 1) by Mg^{2+} ions. The Al occupancies for the other Al sites were 100% to within 3σ. Difference Fourier syntheses calculated at $z = 0{\cdot}138$, 1/6 and 0·180 after the refinement of a model including Al(1), Al(2) (partially occupied by Mg^{2+}), Al(3), Al(4), O(1) to O(5) are reproduced in Fig. 1(*a*)–(*c*). The emergence of the NH_4^+ ion is clearly seen. *Note*: peaks for H atoms are negative (dashed).

Phase 2

The NH_4^+ ions were subsequently included in the $z \sim \frac{1}{6}$ plane with the N atom at a 6(*c*) site, and N—H(1) directed along the negative **c** direction at $x = y = 0$, and along the positive **c** direction at $x = \frac{2}{3}$, $y = \frac{1}{3}$.

---

* See deposition footnote.

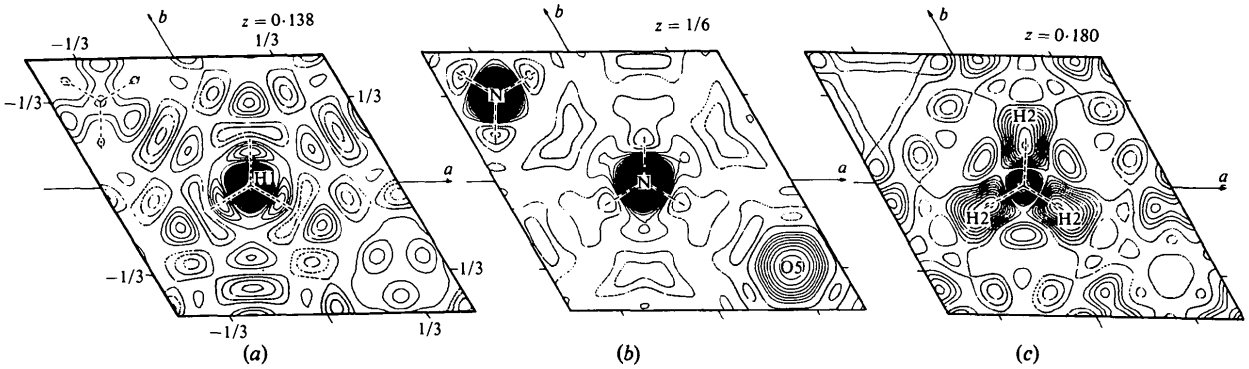

Fig. 1. Difference Fourier syntheses calculated with only O(5) in the conduction plane ($z = \frac{1}{6}$) included in F_c, showing the emergence of the NH_4^+ ion. Sections taken at: (a) $z = 0{\cdot}138$, $\Delta = 0{\cdot}05$ N Å^{-3}; (b) $z = \frac{1}{6}$, $\Delta = 0{\cdot}10$ N Å^{-3}, and (c) $z = 0{\cdot}180$, $\Delta = 0{\cdot}05$ N Å^{-3}.

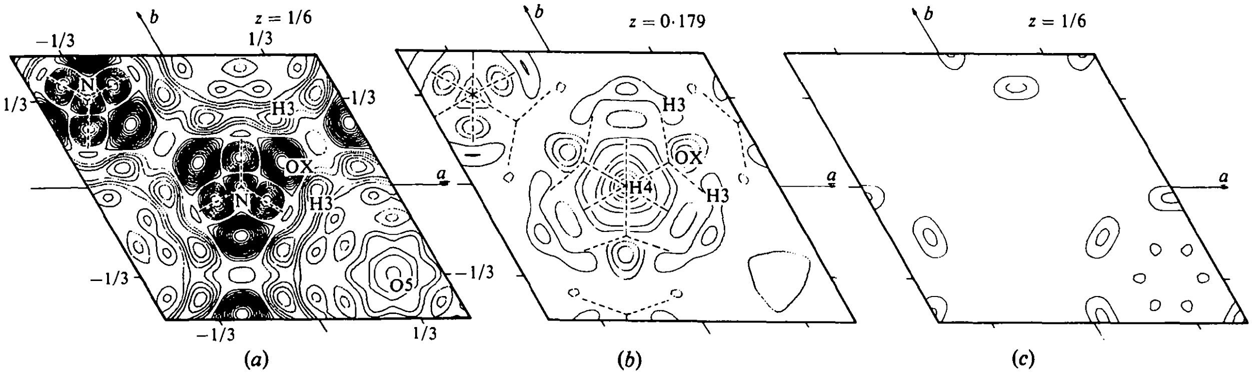

Fig. 2. Difference Fourier syntheses calculated in or near the conduction plane with: (a) O(5) and NH_4 (at $z = \frac{1}{6}$); (b) O(5), NH_4^+, OX and H(3) (at $z = 0{\cdot}179$); and (c) O(5), NH_4^+, OX, H(3) and H(4) (at $z = \frac{1}{6}$) included in the calculation of F_c; $\Delta = 0{\cdot}05$ H Å^{-3} in all three maps.

Constrained refinement of the occupancy for the N, H(1) and H(2) atom positions indicated that the NH_4^+ ion had a site occupancy of 78% (see Table 1). A subsequent difference Fourier synthesis in the $z = \frac{1}{6}$ plane after the inclusion of NH_4^+ is given in Fig. 2(a). Further residual peaks were observed.

Phase 3

The content of Fig. 2(a) was interpreted as O and H density (positive and negative peaks, respectively). Atoms OX and H(3) were included in the refinement for which isotropic temperature factors and non-coupled site occupancies (so as not to bias the interpretation) were refined. A further negative (H-like) peak emerged near $(0,0,\frac{1}{6})$ on the calculation of a difference Fourier synthesis (Fig. 2b). Representing this peak as an additional hydrogen atom H(4), and refining its site occupancy (again uncoupled) and isotropic temperature factor, resulted in a further improvement in R value in the refinement. The interpretation of the resulting arrangement of OX, H(3) and H(4) atoms relies on a number of observations:

(i) The OX—H(3) and OX—H(4) distances [0·859 (3) and 0·947 (9) Å respectively] are of the order of normal O—H bonds in H_2O or H_3O^+.

(ii) The H(3)—OX—H(4) angle [107·9 (9)°] is near the H—O—H angle for H_2O or H_3O^+.

(iii) The site occupation for OX (7·4%) is near to one-third of that for H(4) (22·4%), but greater than that for H(3) (4·4%).

(iv) The sum of the site occupations for H(4) and N after an unconstrained refinement of occupation is almost exactly 100%.

The conclusion is that the arrangement must represent a disordered overlap of H_2O molecules and H_3O^+ ions superposed on the partially occupied NH_4^+ network, as shown schematically in Fig. 3. A trial refinement was therefore made in which $\text{occ}(OX) = \frac{1}{3}\text{occ}(H4) \neq \text{occ}(H3)$, and $B(H4) \neq B(H3) \neq B(OX)$. If α is the fractional site occupation for a given H_2O molecule, and β that for a given H_3O^+ ion, then:

$$2\alpha + \beta = \text{occ}(OX) = \tfrac{1}{3}\text{occ}(H4) = 0{\cdot}0749$$

and

$$\alpha + \beta = \mathrm{occ(H3)} = 0{\cdot}0445,$$

giving $\alpha = 0{\cdot}0304$ and $\beta = 0{\cdot}0141$.

Together with the refined occupation of the Al(2) site by Mg^{2+} (to 38%) and the NH_4^+ site (to 78%), this gives the mean formula unit for the crystal/conducting layer/cell of:

$$(NH_4^+)_{1\cdot55}(H_3O^+)_{0\cdot08}Mg_{0\cdot77}Al_{10\cdot23}O_{17}\cdot(H_2O)_{0\cdot36}.$$

It should be noted that, without any such requirement being imposed on the refinement, this interpretation leads to an almost neutral system (charge imbalance only 0·14 e). That this is reasonable is also suggested by its implication that each vacant NH_4^+ site is fully occupied, either by an H_3O^+ ion in one of three possible orientations or by an H_2O molecule, in one of six possible orientations (Fig. 3).

The final stages of refinement also involved the testing of various anisotropic secondary extinction models. The best agreement was obtained for a type I model using the Becker & Coppens formalism for a Coppens & Hamilton assumed Gaussian mosaic spread (see Becker & Coppens, 1974*a*,*b*, 1975) [$Z'_{11} = 0{\cdot}042\,(3)$, $Z'_{22} = 0{\cdot}064\,(5)$, $Z'_{33} = 0{\cdot}060\,(6)$, $Z'_{12} = -0{\cdot}005\,(4)$, $Z'_{13} = -0{\cdot}010\,(3)$, $Z'_{23} = 0{\cdot}005\,(4)$; $Z_{ij} = Z'_{ij} \times 10^8$]. A check was also made of the occupancies of the O-atom sites: all sites were found to have occupancies insignificantly different from 100%.

A refinement was finally made in which the amount of H_3O^+ in the H_3O^+/H_2O network was constrained to maintain a *neutral* crystal. This gives a final composition of:

$$(NH_4)_{1\cdot56\,(1)}(H_3O^+)_{0\cdot19\,(1)}Mg_{0\cdot75\,(1)}\text{-}$$
$$Al_{10\cdot25\,(1)}O_{17}\cdot(H_2O)_{0\cdot25\,(1)}.$$

The final positional parameters (and fractional occupancies and mean r.m.s. components along the principal axes of the refined vibrational ellipsoids) are given in Table 1. The final agreement factors were $R(F^2) = \sum(|F_o^2| - |F_c^2|)/\sum|F_o^2| = 0{\cdot}035$ and $R_w(F^2) = (\sum w|F_o^2 - F_c^2|^2/\sum w|F_o^4|)^{1/2} = 0{\cdot}049$. The calculated conventional $R(F)$ value was 0·031.

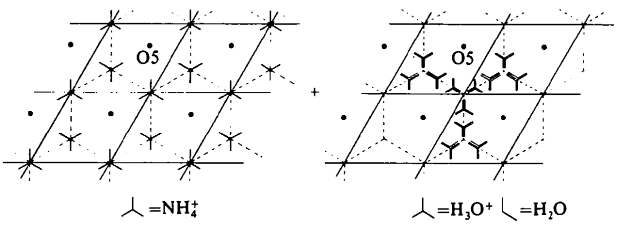

Fig. 3. Schematic representation of the disorder situation in the conduction plane of ammonium–hydronium β''-alumina involving the superposition of a 78% NH_4^+ network and a 22% H_3O^+/H_2O network.

Table 1. *Atomic coordinates* ($\times 10^5$) *and fractional site occupations*

The mean r.m.s. components $\bar{R}$ (Å) along the principal axes of the refined vibrational ellipsoids are also listed.

	x	y	z	Fractional site occupation	$\bar{R}$ ($\times 10^3$)
NH_4^+					
N	0	0	16967 (5)	0·780 (4)	196
H(1)	0	0	13795 (5)		191
H(2)	9042 (36)	$2x$	17997 (9)		316
H_3O^+/H_2O					
O*X*	17257 (142)	$x/2$	16584 (14)	0·073 (2)	116
H(3)	25250 (230)	25845 (246)	17107 (36)	0·052 (2)	193
H(4)	0	0	17847 (41)	0·220 (4)	151
Spinel block					
Al(1)	0	0	0	1·0	69
Al(2)/Mg(2)	0	0	35022 (2)	0.627 (12) Al + 0·373 (12) Mg	72
Al(3)	33622 (11)	$x/2$	6942 (1)	1·0	74
Al(4)	0	0	44925 (3)	1·0	70
O(1)	15364 (4)	$2x$	3355 (1)	1·0	87
O(2)	0	0	29563 (2)	1·0	83
O(3)	0	0	9397 (2)	1·0	79
O(4)	16500 (3)	$2x$	23715 (1)	1·0	80
O(5)	$\frac{1}{3}$	$\frac{2}{3}$	$\frac{1}{6}$	1·0	107

A virtually featureless difference Fourier map (Fig. 2*c*) was obtained after the final refinement.*

Discussion

The spinel block

The structures of the β- and β''-alumina spinel blocks are virtually identical; the only significant difference, apart from their relative orientation in their respective structures, is the Mg^{2+} substitution of certain Al^{3+} sites in the β''-alumina structure. Rigorous systematic refinement of the occupation of the Al sites has given that the only significantly observable Mg^{2+} substitution occurs at the Al(2) site at the centre of the block: 37% of the Al(2) sites are occupied by Mg^{2+} atoms, assuming no vacancies at the site. This is close to the 38% substitution in Na^+ β''-alumina [together with a 4% substitution of the Al(3) site, not observed here] (Roth, Reidinger & La Placa, 1976), and the 34% in Ag^+ β''-alumina (Bates, Brown, Kaneda, Brundage, Wang & Engström, 1979). All three studies combine to dispel the earlier suggestion of Bettman & Peters (1969), made on the basis of electrostatic considerations, that the Mg^{2+} will be found near the conducting planes. The studies also suggest that the size (shape) of the mobile cation (rather than the Mg^{2+} substitution) must be the dominant factor in determining its distribution in the β'' structure. The situation

---

* Details of the crystal size, shape and orientation, a list of structure factors and a table of anisotropic thermal parameters have been deposited with the British Library Lending Division as Supplementary Publication No. SUP 38238 (17 pp.). Copies may be obtained through The Executive Secretary, International Union of Crystallography, 5 Abbey Square, Chester CH1 2HU, England.

Table 2. *Mean* Al(Mg)—O *distances* (Å) *in spinel,* Na^+ *β-,* Na^+ *β″-alumina and here* (*cf. Roth, Reidinger & La Placa,* 1976)

	Coordination	Spinel	$Na^+\beta$	$Na^+\beta''$	NH_4^+/ $H_3O^+\beta''$
Al(1)*	Octahedral	1·929	1·895	1·896	1·891
Al(2)/Mg(2)	Tetrahedral	1·919	1·805	1·849	1·852
Al(3)	Octahedral	1·929	1·918	1·917	1·916
Al(4)	Tetrahedral	1·919	1·745	1·744	1·768

* Atom labels are consistent with the present paper.

can, as has been suggested, be more complicated in the β structure due to the presence there of interstitial O atoms in the conducting layer.

Mean values are given in Table 2 for the Al(Mg)—O distances within the spinel block here and in Na^+ β''-alumina compared to the corresponding distances in Na^+ β-alumina and spinel, $MgAl_2O_4$. Evidence for the role of Mg substitution as a strain reliever at the Al(2) site in the β'' structures is clearly seen: the mean Al—O distance at Al(2) is 2·6% longer here than in Na^+ β-alumina. Some support is also found in this study for the suggestions of Roth *et al.* (1976) that the release of strain at the Al(4) site can be through displacement of the O(5) supporting oxygen in the conduction plane: the r.m.s. vibrational amplitude in the conducting plane $(\overline{U_{11}^2})^{1/2}$ is here 0·127 (8) Å, while perpendicular to the plane $(\overline{U_{33}^2})^{1/2}$ is 0·068 (3) Å. The corresponding values in Na^+ β''-alumina were 0·218 and 0·068 Å. The smaller value in the conduction plane in the present case can reflect that O(5) is here held more tightly (by weak H bonds from the NH_4^+ ions) or, alternatively, that the Al(4)—O(5)—Al(4) bridge is more stretched.

The conduction layer

It should first be noted that although a true conduction plane exists in the β-alumina structure this is not the case for the β'' structure. Here the N atoms of the NH_4^+ ions 'undulate' from ~0·1 Å above to ~0·1 Å below the mean conduction planes at $z = \pm\frac{1}{6}$ and $\frac{1}{2}$. This effect will be neglected for discussion purposes: all plots have been made in the $z = \frac{1}{6}$ plane. For conceptual simplicity, the mobile components of the conducting plane (NH_4^+, H_3O^+ and H_2O) will first be considered separately.

The NH_4^+ *ion.* The $6(c)$ sites of the conduction plane were found to be occupied to 78% by NH_4^+ ions. An implication of the symmetry centre at the $9(d)$ site is that each NH_4^+ ion [at a $6(c)$ site] with one of its N—H bonds [N—H(1)] pointing along the **c** direction is surrounded by three NH_4^+ ions with their N—H(1) bonds pointing in the opposite direction. The remaining N—H bonds all lie on mirror planes with H(2) occupying $18(h)$ sites. The geometry of the NH_4^+ ion is given in Table 3, and the arrangement in the conducting plane is shown schematically in Fig. 3. It is seen that the NH_4^+ ion is strongly hydrogen-bonded along the c axis to O(3), with an N—H(1)···O(3) distance of 2·602 (2) Å. Weaker hydrogen bonds are also made to O(4) and O(5).

The H_3O^+/H_2O *network.* The superposition of H_3O^+ ions or H_2O molecules which occupy the NH_4^+ vacancies (only 22% of the NH_4^+ sites) is illustrated schematically in Fig. 3.

The refined geometry (Table 3 and Fig. 4) is reasonable considering that the atomic arrangement represents a statistical overlap of H_3O^+ and H_2O units, *e.g.* the H(4) site is occupied by an overlap of H atoms belonging to H_3O^+ and H_2O units; this overlap is not exact in practice.

It is of relevance here to consider the instantaneous short-range structural situation of the individual H_3O^+ and H_2O units (Figs. 3 and 4). We see that, in the conduction plane, the H_3O^+ ions and H_2O molecules

Table 3. *Some distances* (Å) *and angles* (°)

(*a*) Al—O distances			
Al(1)—O(1)	1·891 (1) × 6	Al(3)—O(2)	1·946 (1) × 1
Al(2)/Mg(2)—O(1)	1·844 (1) × 3	Al(3)—O(1)	1·999 (1) × 2
Al(2)/Mg(2)—O(2)	1·877 (1) × 1	Al(4)—O(5)	1·745 (1) × 1
Al(3)—O(3)	1·844 (1) × 1	Al(4)—O(4)	1·776 (1) × 3
Al(3)—O(4)	1·855 (1) × 2		
(*b*) NH_4^+ ion			
N—H(1)	1·091 (2) × 1	H(1)—N—H(2)	111·9 (2)
N—H(2)	0·950 (3) × 3	H(2)—N—H(2)	107·0 (2)
(*c*) H_3O^+/H_2O network (see Fig. 4)			
O*X*—H(3)	0·859 (13)	H(3)—O*X*—H(3)	120·2 (18)
O*X*—H(4)	0·947 (9)	H(3)—O*X*—H(4)	107·9 (9)
H(2)···H(3)	1·692 (11)		
N···O*X*	2·411 (7)		
H(2)···O*X*	2·155 (7)		

(*d*) Hydrogen bonds

X—H···*Y*	*X*···*Y*	*X*—H	H···*Y*	*X*—H···*Y*
N—H(1)···O(3)	2·602 (2)	1·091 (2)	1·512 (2)	180·0
N—H(2)···O(4)	2·823 (2)	0·950 (3)	2·096 (3)	132·2 (3)
N—H(2)···O(5)	3·252 (1)	0·950 (3)	2·413 (4)	147·2 (2)
O*X*—H(3)···O(5)	2·923 (2)	0·859 (13)	2·114 (12)	156·8 (12)
O*X*—H(3)···O(4)	2·820 (4)	0·859 (13)	2·401 (12)	110·5 (9)
··O(4)	3·467 (4)	0·947 (9)	2·580 (11)	155·9 (10)
O*X*—H(4)···O(4)	2·820 (4)	0·947 (9)	2·580 (11)	94·7 (6)
··O(4)	2·820 (4)	0·947 (9)	2·580 (11)	94·7 (6)

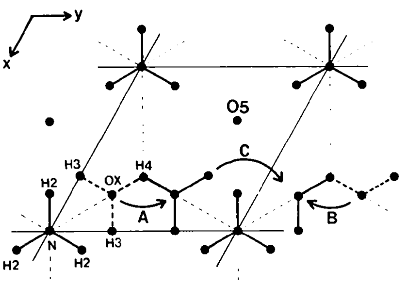

Fig. 4. A typical 'instantaneous' short-range situation in the conduction plane of ammonium–hydronium β''-alumina. The arrows *A*, *B* and *C* represent schematically the basic components of the proposed proton-transfer mechanism (see text). See also Table 3 for some distances and angles relevant to the figure.

each have H atoms directed towards the column oxygen O(5): the H···O distances for the weak in-plane OX–H(3)···O(5) bonds and even weaker OX–H(3)···O(4) bonds are 2·114 (2) and 2·401 (12) Å, respectively; H(4) interacts very weakly with three equivalent O(4) atoms at H···O distances of 2·580 (11) Å. That OX does not also occupy a 6(c) site (as does the N atom) must imply that the effective electrostatic potential within an NH_4^+ vacancy favours a lower site symmetry for the H_3O^+ and H_2O units than that consistent with a more central OX position. The point symmetry of the NH_4^+ ion facilitates an ordering of its equilibrium position through the formation of the strong N–H(1)···O(3) bond. It is nonetheless somewhat surprising that OX–H bonds do not form in the NH_4^+ vacancies to overlap roughly with the N–H(1) bond positions, and so produce short OX–H···O(3) bonds to the spinel block. It may be that the hydrogen-bond-accepting capacity of the 'surfaces' of the spinel blocks which form the boundaries of the conducting layer is exhausted by the strong N–H···O bonds from the NH_4^+ ion to expose a surface of more hydrophobic character at the NH_4^+ vacancies. This would help to explain the considerably higher ionic conductivity (to be discussed later) in NH_4^+–H_3O^+ β''-alumina compared to that for the pure H_3O^+ β''-alumina system. In the latter case, the H_3O^+ ions can (and presumably do) avail themselves, in the absence of NH_4^+ ions, of the full hydrophilic character of the spinel blocks in forming hydrogen bonds to them. These would have the dual effect of both 'braking' the translational motion of the H_3O^+ ions, and hindering the formation of an efficient Grotthus network in the conduction layers – so limiting the ionic conductivity. The detailed D_3O^+ β''-alumina structure is under current investigation by the present authors using single-crystal neutron diffraction techniques. A recent elastic and inelastic neutron diffraction study of H_3O^+ β''-alumina (Roth, Anne & Tranqui, 1980) is inconclusive with regard to the possible microscopic proton-transfer mechanism.

The conduction mechanism

As mentioned earlier, ammonium–hydronium β''-alumina has a conductivity that is unusually high for a protonic solid electrolyte. The conductivity of the particular composition $(NH_4)_{1\cdot00}(H_3O)_{0\cdot67}Mg_{0\cdot67}Al_{10\cdot33}O_{17}$ is about 10^{-3} Ω^{-1} cm^{-1} at 298 K. It increases with an activation energy of 0·3 eV to 6×10^{-3} Ω^{-1} cm^{-1} at 463 K. This composition has the highest conductivity reported of any of the protonic β- or β''-aluminas. For comparison, the conductivity of NH_4^+ β-alumina is $1\cdot3 \times 10^{-6}$ Ω^{-1} cm^{-1} at 298 K and $8\cdot0 \times 10^{-4}$ Ω^{-1} cm^{-1} at 473 K ($E_a = 0\cdot47$ eV), and that of H_3O^+ β-alumina is about 10^{-11} Ω^{-1} cm^{-1} at 298 K and 8×10^{-7} Ω^{-1} cm^{-1} at 473 K ($E_a = 0\cdot78$ eV). Although the conductivity of H_3O^+ β''-alumina has not been measured unambiguously as a function of water content, preliminary reports show it to be much higher than that of H_3O^+ β-alumina, probably in the range $\sigma \sim 10^{-5}$ to 10^{-3} Ω^{-1} cm^{-1} at 298 K. In general, protonic β''-aluminas are more conductive than their β-alumina counterparts.

It is conceivable that charge in ammonium–hydronium β''-alumina is carried by the diffusion of NH_4^+ and H_3O^+ ions, as well as by H^+ transfer through an H_3O^+/H_2O network. Because an understanding of the properties of ammonium–hydronium β''-alumina requires consideration of all these proton-conduction mechanisms, its structure is important not only for what it concludes about this particular composition, but also for what it indicates about diffusion in pure ammonium and pure hydronium β''-alumina. In the following sections we discuss the diffusion of NH_4^+, H_3O^+ and H^+ in β''-alumina.

NH_4^+ *diffusion*

In NH_4^+–H_3O^+ β''-alumina, NH_4^+ is strongly bonded along the c axis to O(3) through a single hydrogen bond with the extremely short N–H(1)···O(3) distance of 2·602 (2) Å. Weaker hydrogen bonds are formed to the three O(5) atoms surrounding the 6(c) sites. NH_4^+ ions may be immobile, rotate around the N–H(1)···O(3) bond, or translate through the structure. Translational motion should be greatly hindered by the strength of the N–H(1)···O(3) bond. The specific motions occurring at a given temperature will depend on the relative energies of the hydrogen bonds, as well as on other factors which influence the activation energy for diffusion. Evidence of local NH_4^+ rotation around N–H(1)···O(3) and NH_4^+ translation has already been seen in NMR measurements (Ochadlick, Bailey, Stamp, Story, Farrington & Briant, 1979).

The preparation of ammonium–hydronium β''-alumina surely involves the diffusion of NH_4^+ species in the structure. However, the extent to which NH_4^+ motion contributes significantly to conductivity in various ammonium–hydronium β''-alumina compositions may well depend most critically on whether sufficient H_3O^+ and H_2O species are present in a particular crystal to establish a long-range Grotthus diffusion pathway for H^+.

The conductivity of the one ammonium–hydronium β''-alumina sample which has been measured, of nominal composition $(NH_4)_{1\cdot00}(H_3O)_{0\cdot67}Mg_{0\cdot67}Al_{10\cdot33}O_{17}$, is extremely high; but, perhaps more significantly, its activation energy (0·3 eV) is much lower than the activation energy for conductivity in ammonium β-alumina (0·5 eV). Ammonium ions are strongly hydrogen-bonded to the O framework of both structures. If the critical barrier to NH_4^+ diffusion is the hydrogen-bond energy, it is reasonable to expect that the conductivity of ammonium β''-alumina might well be as low as that of ammonium β-alumina, and that the activation energy for conductivity in ammonium β''-alumina would be closer to 0·5 eV than 0·3 eV. The much higher conductivity and lower activation energy observed in mixed ammonium–hydronium β''-alumina, therefore, may well signal that its conductivity occurs predominantly through Grotthus H^+ motion, and that the transport number of NH_4^+ is quite small.

H_3O^+ *conduction and the Grotthus mechanism*

The central question in considering conduction in any of the hydrated β- and β''-aluminas is that of whether charge is transported primarily through a Grotthus network or by H_3O^+ diffusion. It has, in fact, proved possible to derive a Grotthus-type mechanism from the disordered structure shown in Fig. 3. This average picture is, of course, misleading in discussing the H^+ conduction mechanism. The actual short-range structural situation is that each NH_4^+ vacancy is occupied *either* by an H_2O molecule in one of its six possible orientations *or* by an H_3O^+ ion in *one* of its three possible orientations. There is roughly a 4:3 ratio of H_2O to H_3O^+ units. With this picture in mind, and conscious of the possible role of NH_4^+ rotation as an ion-diffusion enhancement factor, a simple model for the proton-transfer mechanisms is readily imagined, which represents the familiar Grotthus-type H^+ transfer mechanism involving the following three components:

(*a*) A 120° rotational flip of an H_3O^+ ion within the conducting plane about the hexagonal axis through H(4) (*A* in Fig. 4).

(*b*) Rotation of an H_2O molecule either about H(4) in the conducting plane (*B* in Fig. 4), or about O*X*–H(4) to a position capable of receiving a proton to create an H_3O^+ ion.

(*c*) Transport of the proton (*C* in Fig. 4) from the H_3O^+ ion of (*a*) to the H_2O molecule of (*b*) through the linked toroid-like hexagonal regions in the conducting plane surrounding each supporting oxygen atom O(5). The proton-jump distance illustrated in Fig. 4 is 1·39 (2) Å.

An intriguing suggestion emerging from this structural analysis is then that movement of protons around O(5) oxygens may be an important step in any Grotthus mechanism in the β''-alumina structure.

This Grotthus mechanism may or may not contribute significantly to conductivity in the particular ammonium–hydronium β''-alumina composition $[(NH_4)_{1\cdot56}(H_3O)_{0\cdot19}Mg_{0\cdot75}Al_{10\cdot25}O_{17}.(H_2O)_{0\cdot25}]$ whose structure has been determined in this study. The low concentrations of H_3O^+ and H_2O make the existence of a network of donor–acceptor groups throughout the crystal uncertain. The only ammonium–hydronium β''-alumina composition for which conductivity has been determined has a much higher H_3O^+ and H_2O content $[(NH_4)_{1\cdot00}(H_3O)_{0\cdot67}Mg_{0\cdot67}Al_{10\cdot33}O_{17}]$.

This difference in composition also makes it difficult to relate this work to the French work in this field (see, for example, Colomban & Novak, 1981, and references therein). Indeed, the general picture now emerging of protonic β- and β''-aluminas is one of considerably greater complexity than was at first appreciated. Future work must pay strict attention to specimen characterization to avoid subsequent ambiguities in the interpretation of composition, conductivity and structure work.

Recent quasi-electric neutron scattering (QNS) studies have been performed on NH_4^+ β-, NH_4^+ β''- and $NH_4^+/H^+(H_2O)_n$ β''-alumina single crystals at elevated temperatures (Colomban, Lassegues & Baffier, 1982) with a view to observing line-broadening effects related to translational and rotational motions in these compounds. No significant broadenings have been observed, however. This does not eliminate the possibility that an efficient Grotthus network is formed over a narrow range of water content (not as yet studied in the QNS experiments), and that, within this region, the proton conductivity rises sharply. This critical-water-content effect may be the case in the $NH_4^+/H^+(H_2O)_n$ β''-alumina system reported here.

At the University of Pennsylvania this research was supported by the Department of Energy under Grant No. DE-ACO28OER10597. The work carried out at the Department of Chemistry, University of Uppsala, is supported by grants from the Swedish Natural Science Research Council.

References

BATES, J. B., BROWN, A. M., KANEDA, T., BRUNDAGE, W. E., WANG, J. C. & ENGSTRÖM, H. (1979). *Fast Ionic Transport in Solids*, edited by P. VASHISHTA, J. N. MUNDY & G. K. SHENOY, p. 261. New York: North-Holland.

BECKER, P. J. & COPPENS, P. (1974*a*). *Acta Cryst.* A**30**, 129–147.

BECKER, P. J. & COPPENS, P. (1974*b*). *Acta Cryst.* A**30**, 148–153.

BECKER, P. J. & COPPENS, P. (1975). *Acta Cryst.* A**31**, 417–425.

BETTMAN, M. & PETERS, C. R. (1969). *J. Phys. Chem.* **93**, 1774–1780.

BREITER, M. W., FARRINGTON, G. C., ROTH, W. L. & DUFFY, J. L. (1977). *Mater. Res. Bull.* **12**, 895–906.

BRIANT, J. L. & FARRINGTON, G. C. (1981). *J. Electrochem. Soc.* **128**, 1830–1834.

COLOMBAN, PH., LASSEGUES, J. C. & BAFFIER, N. (1982). Private communication.

COLOMBAN, PH. & NOVAK, A. (1981). *Solid State Ionics*, **5**, 241–244.

FARRINGTON, G. C. & BRIANT, J. L. (1978). *Mater. Res. Bull.* **13**, 763–773.

FARRINGTON, G. C. & BRIANT, J. L. (1979). *Fast Ionic Transport in Solids*, edited by P. VASHISHTA, J. N. MUNDY & G. K. SHENOY, p. 395. New York: North-Holland.

FARRINGTON, G. C., BRIANT, J. L., BREITER, M. W. & ROTH, W. L. (1978). *J. Solid State Chem.* **24**, 311–319.

HOOPER, A., TOFIELD, B. C. & SAMPSON, C. F. (1979). *Fast Ionic Transport in Solids*, edited by P. VASHISHTA, J. N. MUNDY & G. K. SHENOY, p. 409. New York: North-Holland.

International Tables for X-ray Crystallography (1974). Vol. IV. Birmingham: Kynoch Press.

LEHMANN, M. & LARSEN, F. K. (1974). *Acta Cryst* A**30**, 580–584.

LUNDGREN, J.-O. (1979). *Crystallographic Computer Programs*. Report UUIC-B13-4-04. Inst. of Chemistry, Univ. of Uppsala, Sweden.
OCHADLICK, A. R., BAILEY, W. C., STAMP, R. L., STORY, H. S., FARRINGTON, G. C. & BRIANT, J. L. (1979). *Fast Ionic Transport in Solids*, edited by P. VASHISHTA, J. N. MUNDY & G. K. SHENOY, p. 401. New York: North-Holland.
PETERS, C. R., BETTMAN, M., MOORE, J. W. & GLICK, M. D. (1971). *Acta Cryst.* B**27**, 1826–1834.
POTIER, A. & ROUSSELET, D. (1973). *J. Chim. Phys. Phys. Chim. Biol.* **70**, 873–878.
ROTH, W. L. (1972). *J. Solid State Chem.* **4**, 60–75.
ROTH, W. L., ANNE, M. & TRANQUI, D. (1980). *Rev. Chim. Minér.* **17**, 379–396.
ROTH, W. L., BREITER, M. W. & FARRINGTON, G. C. (1978). *J. Solid State Chem.* **24**, 321–330.
ROTH, W. L., REIDINGER, F. & LA PLACA, S. (1976). *Superionic Conductor*, edited by G. D. MAHAN & W. L. ROTH, p. 223. New York: Plenum.
SHILTON, M. G. & HOWE, A. T. (1977). *Mater. Res. Bull.* **12**, 701–706.
SHILTON, M. G. & HOWE, A. T. (1979). *Fast Ionic Transport in Solids*, edited by P. VASHISHTA, J. N. MUNDY & G. K. SHENOY, p. 730. New York: North-Holland.

Acta Cryst. (1983). B**39**, 235–238

[Fe_4Te_8]-Cluster in $Cs_7Fe_4Te_8$;* ein Neuartiges Bauprinzip bei Ternären Metallchalkogeniden

VON WELF BRONGER, MANFRED KIMPEL UND DIETER SCHMITZ

Institut für Anorganische Chemie der Technischen Hochschule Aachen, D-5100 Aachen, Bundesrepublik Deutschland

(*Eingegangen am* 7. *September* 1982; *angenommen am* 25. *Oktober* 1982)

Abstract

The crystal structure of $Cs_7Fe_4Te_8$ has been determined by single-crystal X-ray techniques. The crystals are monoclinic, $C2/c$, with $a = 20{\cdot}569\,(6)$, $b = 9{\cdot}306\,(3)$, $c = 18{\cdot}235\,(4)$ Å, $\beta = 117{\cdot}48\,(2)°$ and $Z = 4$. Full-matrix least-squares refinement of 1595 independent observed reflexions gave a conventional R index of 0·038. The atomic arrangement $[Cs_7(Fe_4)]Te_8$ corresponds to that in cesium chloride. The outstanding feature of the crystal structure is the occurrence of isolated $[Fe_4Te_8]$ clusters, in which the Fe atoms are tetrahedrally surrounded by Te atoms and four tetrahedra are mutually linked such that each is joined to the others *via* three edges, corresponding to $[FeTeTe_{3/3}]_4$.

1. Einleitung

Die Kristallstrukturen der bekannten Alkalithio- bzw. -selenoferrate sind charakterisiert durch kantenverknüpfte, mit Eisenatomen zentrierte Chalkogentetraeder. Dabei werden in den Strukturen der Verbindungen $AFeX_2$ mit $A \triangleq$ K, Rb oder Cs und $X \triangleq$ S oder Se Ketten, entsprechend dem Schema ${}^1_\infty[FeX_{4/2}]$, ausgebildet. Die Strukturen der Natriumverbindungen Na_3FeS_3 und Na_3FeSe_3 (Müller & Bronger, 1981) enthalten isolierte Doppeltetraeder, $[FeX_{2/2}X_2]_2$.

Uns gelang jetzt die Darstellung von $Cs_7Fe_4Te_8$ (Bronger, Kimpel & Schmitz, 1982), einer Verbindung mit isolierten $[Fe_4Te_8]$-Baugruppen, die, entsprechend dem Schema $[FeTe_{3/3}Te]_4$, wiederum durch kantenverknüpfte, mit Eisenatomen zentrierte Chalkogentetraeder aufgebaut sind.

2. Durchführung der Experimente

Synthese

Die Darstellung des Caesiumtelluroferrats erfolgte durch Umsetzung von Gemengen aus Eisen und Caesiumcarbonat in einer Tellur–Wasserstoff-Atmosphäre.

Die Versuche wurden in einem Quarzrohr ausgeführt, das mittels eines elektrischen Röhrenofens beheizt wurde. Ein Korundschiffchen nahm das Gemenge aus Eisenpulver (Firma Zinsser, angegebener Reinheitsgrad 99,96%) und Caesiumcarbonat (Firma Merck, angegebener Reinheitsgrad 99,5%) im molaren Verhältnis 1:2 auf und wurde in eine Zone des Ofens gebracht, die eine konstante Temperatur von etwa 1050 K hatte. Ein zweites, mit Tellurpulver (Firma Merck, angegebener Reinheitsgrad 99%) beschicktes Korundschiffchen wurde etwa 20 cm vor dem ersten Schiffchen, gegen die Strömungsrichtung

---

* Heptacaesium-tetraeisen-octatellurid.

0567-7408/83/020235-04$01.50